ACS OMEGA

Open Access

http://pubs.acs.org/journal/acsodf

Article

Laboratory Studies of the Clathrate Hydrate Formation in the Carbon Dioxide-Water Mixtures at Interstellar Conditions

Aliya Tychengulova,* Karakoz Katpayeva, Saule Shomshekova, Saltanat Ibragimova, Oleg Golikov, Darkhan Yerezhep,* Dmitriy Sokolov, and Abdurakhman Aldiyarov

Cite This: *ACS Omega* 2025, 10, 1237−1248

Read Online

ACCESS | Metrics & More | Article Recommendations

ABSTRACT: This study investigates the formation of carbon dioxide clathrate hydrates under conditions simulating interstellar environments, a process of significant astrophysical and industrial relevance. Clathrate hydrates, where gas molecules are trapped within water ice cages, play an essential role in both carbon sequestration strategies and understanding of the behavior of ices in space. We employed a combination of Fourier Transform Infrared (FTIR) spectroscopy, mass spectrometry, temperature-programmed desorption (TPD), and Density Functional Theory (DFT) calculations to explore thin films of H_2O:CO_2 ice mixtures with varying CO_2 concentrations (5−75%) prepared by vapor deposition at temperatures ranging between 11 and 180 K. The study revealed the influence of CO_2 concentration and deposition temperature on the formation mechanism of diverse structures, including clathrate hydrates, polyaggregates, and segregated CO_2 groups. Spectral features associated with CO_2 encapsulation in clathrate hydrates were observed at 2335, 2349, and 3698 cm^{-1} in the 5 and 15% mixtures after deposition at 11 K and after warming at temperatures above 100 K. The observed increase in CO_2 sublimation temperature to 145−155 K and co-condensation of CO_2 molecules at 172 K with water molecules at a pressure of 0.5 μTorr can be attributed to the encapsulation of CO_2 molecules within the robust hydrogen-bonded framework of the clathrate cages under specific conditions. These findings enhance our understanding of the intricate processes involved in clathrate and hydrate formation in CO_2 and H_2O mixtures, shedding light on their physical properties and the dependence of their specific characteristics on the formation method.

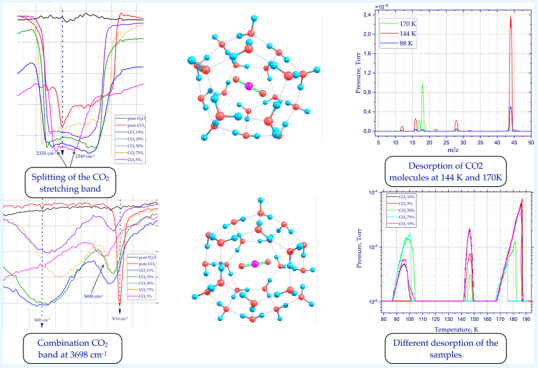

INTRODUCTION

Studying the CO_2 structure and spectroscopic properties has essential astrophysical implications since carbon dioxide is present in various forms in solar system bodies and interstellar ice mantles.[1−5] CO_2 ice exhibits a variety of forms and spectral behaviors depending on factors such as temperature, pressure, and interactions with other molecules like water. Ahrens et al.[4] reviewed the diverse nature of CO_2 ice across the outer Solar System, highlighting its tendency to mix with other species like CH_4 and N_2, forming clathrate hydrates or other complex mixtures. Yu et al.[3] compiled a database of thermodynamic and physical properties for various organic molecules, including CO_2, emphasizing the importance of accurate data for modeling physical processes on Titan and other icy bodies. Detailed investigations of the spectroscopic features associated with different physical states of CO_2 ice are essential for understanding the composition, thermal history, and potential habitability of celestial objects. Vibrational bands of CO_2 ice formed at different temperatures and pressures have been the subject of many experimental works[6−12] since IR spectroscopy is an essential tool for the remote sensing observations of astrophysical objects.

There are numerous works that consider CO_2 mixtures with different substances, such as H_2O and CH_3OH.[6,9,10,13] This is necessary to explain the shifts of the IR peaks and understand the structure of the objects better. The resulting spectra are characterized by broadening and red shifting of the CO_2 features[10,13] due to the interaction between the mixing molecules. These works report main spectral variations at temperatures above 50−60 K, defined as the consequence of the molecular segregation from the water ice. Öberg et al.[11] demonstrated that molecules tend to form segregated groups in binary mixtures (CO_2:H_2O) as long as it is more favorable

Received: September 25, 2024
Revised: November 26, 2024
Accepted: December 11, 2024
Published: December 23, 2024

to interact with similar molecules. Additionally, they found thickness and compositional dependence.

The infrared fingerprints of carbon dioxide have also been extensively studied in the form of clathrate hydrates using infrared transmission spectroscopy,[8,14] attenuated total reflection spectroscopy,[15] and reflection spectra for CO_2 ice or CO_2 clathrate hydrates.[16−18] While clathrate hydrates generally exist under high-pressure conditions, their potential existence in the interstellar medium has garnered increasing attention. Early studies by Sandford and Allamandola[19] suggest the presence of clathrates at low temperatures. Blake et al.[20] demonstrated that clathrates with a type II structure entrapping CO_2 and CH_3OH are formed upon warming the vapor-deposited samples up to 120 K. Fleyfel and Devlin[14] investigated the clathrate of type I and II structures formation in a vacuum chamber using epitaxial growth. More recently, the transformation of vapor-deposited amorphous ice into CO_2 clathrate hydrates after warming the mixtures to the temperatures above the 100 K was observed by Netsu and Ikeda-Fukazawa.[21] Ghosh et al.[22] observed the IR signatures of CO_2 clathrates deposited at 10 K and annealed at 120 K for 48 h at a pressure of 10^{-10} mbar. They also highlighted the dynamic nature of clathrate hydrates under ultrahigh-vacuum and cryogenic conditions, revealing the migration of CO_2 from clathrate cages to the amorphous solid water matrix in the presence of tetrahydrofuran.[23] Ghosh et al.[24] further summarized research on the formation, transformation, and kinetics of clathrate hydrates under simulated interstellar conditions. It was shown that various clathrate hydrates can be formed at extremely low temperatures and pressures. While Schiltz et al.[5] identified distinct spectral features associated with different physical states of CO_2 ice, they attributed the observed spectral features to porous structure and band broadening rather than clathrate hydrate formation. This highlights the ongoing debate and the need for further investigation into the nature of CO_2 ice in astrophysical environments. In this work, we report the formation of carbon dioxide clathrate hydrates under conditions similar to interstellar media using FTIR and mass spectroscopic tools for vapor-deposited thin films of CO_2:H_2O ice mixtures. We considered concentration and temperature variations and their influence on clathrate formation. In addition, we intended to calculate within the first-principles approach the IR signatures of several structural models for the CO_2:H_2O ice mixtures to facilitate the comparison and tentative interpretation of the experimental observations.

While our current study focuses on the thermodynamic and spectroscopic properties of CO_2 hydrates formed under simulated interstellar conditions, we acknowledge that the water-CO_2 flow rate ratio can influence the kinetics and efficiency of hydrate formation, particularly in natural environments and industrial applications. Future studies incorporating flow rate as a key parameter suggested by the literature[25−29] could provide a more comprehensive understanding of the hydrate formation process.

RESULTS AND DISCUSSION

Vibrational Spectroscopy. We studied the infrared absorption bands of icy films containing molecules of astrophysical interest and their interactions in the mixture. Here, we have presented the results relative to the profile of CO_2 absorption bands in an icy mixture of H_2O:CO_2. Figure 1 shows the mid-IR spectrum of H_2O:CO_2 mixtures with

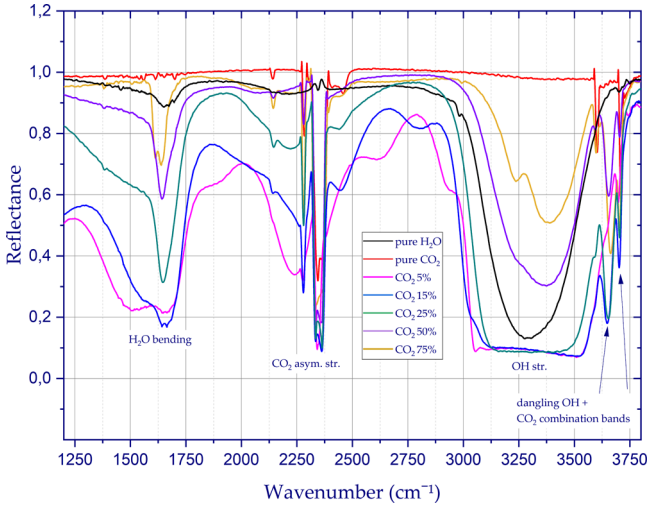

Figure 1. FTIR spectra of CO_2:H_2O mixtures at different concentrations compared to pure water and carbon dioxide at 11 K.

different concentrations at 11 K compared to the mixture's components in their pure forms. The broad, strong absorptions at 3288 and 1658 cm^{-1} can be assigned to pure amorphous solid H_2O.[19,30] The sharp mid-IR peaks of pure CO_2 appear at 2283.5 and 2341 cm^{-1}.[7,30] The shorter wavelength, less intense, near-IR absorptions of CO_2 are found at 3601 and 3710 cm^{-1}. The absorption band at around 2341 cm^{-1} that dominates the mid-IR range corresponds to the asymmetric stretch of CO_2.

Figure 1 shows that IR spectra of CO_2 in H_2O at low temperatures are broader and red-shifted by 10−15 cm^{-1} than those of pure CO_2 under the same conditions. The spectra are also characterized by the essential effect on the OH stretching vibrational band at around 3285 cm^{-1}. The presence of 50 and 75% CO_2 molecules in the mixture causes a strong blueshift of 91 and 100 cm^{-1}, respectively. However, the OH stretching band at lower concentrations of CO_2 experiences significant broadening up to the values of full width at half-maximum (fwhm) of 610 cm^{-1} compared with 438 cm^{-1} for pure H_2O. Moreover, CO_2 in H_2O produces new absorptions that are not present (or greatly diminished) in the spectra of the pure materials. We discuss each of these features in more detail below.

Figure 2 shows the region 3750−3550 cm^{-1} of pure CO_2 and H_2O compared with the spectra of H_2O:CO_2 ice mixtures of different concentrations at 11 K. The two peaks at 3702 and 3601 cm^{-1} can be attributed to the $\nu_1 + \nu_3$ and $2\nu_2 + \nu_3$ combination modes of CO_2, respectively.[30] The absorption of CO_2 in solid H_2O is characterized by significantly broader bands compared to pure solid CO_2. An interesting feature is found around 3650 cm^{-1}, which is identified in the literature[31] as the dangling OH of H_2O. This band is usually observed in mixtures with H_2O and is explained by the disruption of the hydrogen bond network due to the inclusion of the guest molecule. Notably, this band is absent in the mixture with the lowest concentration of CO_2 (5%), which could be explained by the fact that the molecules are already trapped inside the clathrates during the deposition at 11 K. Furthermore, a shift in the position of this band depending on the concentration reflects the differences in formed structures and interactions. Wider, prominent bands from H_2O:CO_2 = 85:15% and H_2O:CO_2 = 75:25% could arise from the interaction of

https://doi.org/10.1021/acsomega.4c08342
ACS Omega 2025, 10, 1237−1248

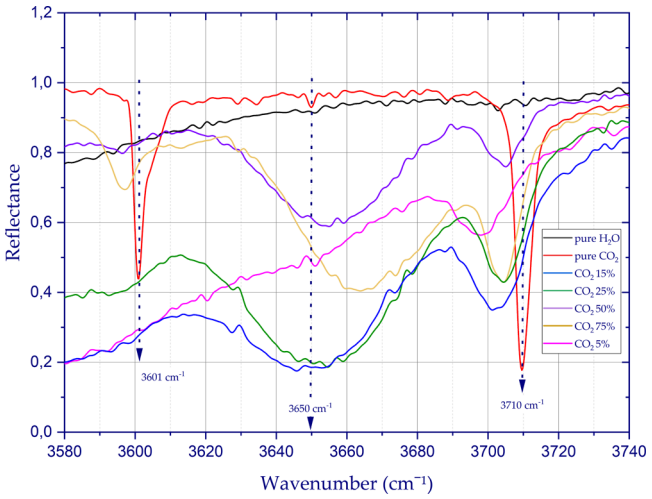

Figure 2. FTIR spectra of H_2O:CO_2 mixtures with different concentrations deposited at 11 K.

water with compact polyaggregates of varied sizes. Band sharpening for the mixtures with 50 and 75% CO_2 could correspond to large CO_2 groups resembling the crystal structure of pure carbon dioxide molecules.

In addition, the red shift toward 3698 cm^{-1} for the combination band at around 3710 cm^{-1} is stronger for the 5% mixture than for other mixtures, possibly due to the guest–host interactions of CO_2 inside the cage. It is also worth mentioning that the spectral feature at 3601 cm^{-1} in the mixtures is diminished for all concentrations of CO_2 except for 75% which could arise from the fact that segregated groups of CO_2 are already formed during deposition. However, the peak at 3710 cm^{-1} is well resolved in the spectra of all the species, although with the shift.

Figure 3a displays the temperature dependence of the 3710 and 3650 cm^{-1} absorption bands of H_2O:CO_2 = 85:15% ice deposited at 11 and at 40 K warmed up to 180 K. Sharp peaks consistent with pure CO_2 are superimposed on the broader absorptions from CO_2 in H_2O. The band associated with the dangling OH bonds becomes sharper and less intense until it entirely diminishes at 145 K.

The more substantial redshift of the CO_2 combination band at 11 K at around 3702 cm^{-1} and the diminished band around 3650 cm^{-1} (as observed for the 5% mixture) can indicate the formation of clathrates in such conditions. The broad prominent band observed at 11 K could correspond to the regions of CO_2 molecules trapped inside the H_2O clathrates and interactions between small CO_2 polyaggregates of various sizes with the host molecules. Upon warming, increased molecular mobility leads to the integration of the separate polyaggregates into isolated CO_2 groups trapped in water pores, which then slowly sublimate coupled with water molecules at temperatures above 145 K.

Comparing Figure 3a,b reveals distinct structures formed at 11 and 40 K. The peak shapes and their changes upon warming indicate different formation and sublimation mechanisms. The higher sublimation temperature (at 155 K) for the mixtures deposited at 11 K as well as the band observed around 3698 cm^{-1} at 145 K further supports the presence of clathrates. In the samples deposited at 40 K, the sharper bands at 3650 and 3702 cm^{-1} and the sublimation of most CO_2 molecules by 100 KK indicate the formation of isolated groups within the pores. These groups, which resemble crystalline peaks at 90 K, readily sublimate at lower temperatures.

It is well-known that H_2O is observed in its amorphous solid water (ASW) form under interstellar conditions and can trap small molecules. The phenomenon of a significant rise in the sublimation temperature of CO_2 in H_2O mixtures is generally interpreted in literature[9−15] as sealing off the pores and releasing the trapped molecules within the ice because of the structural rearrangements that occur during the amorphous to crystalline phase transition at around 150 K. In the course of this research, we observed a similar formation of isolated CO_2 groups trapped inside the water pores in the 15% CO_2 concentration samples deposited at 40 K.

Figure 3b demonstrates the temperature-dependent changes in the dangling OH band and the CO_2 combination bands for

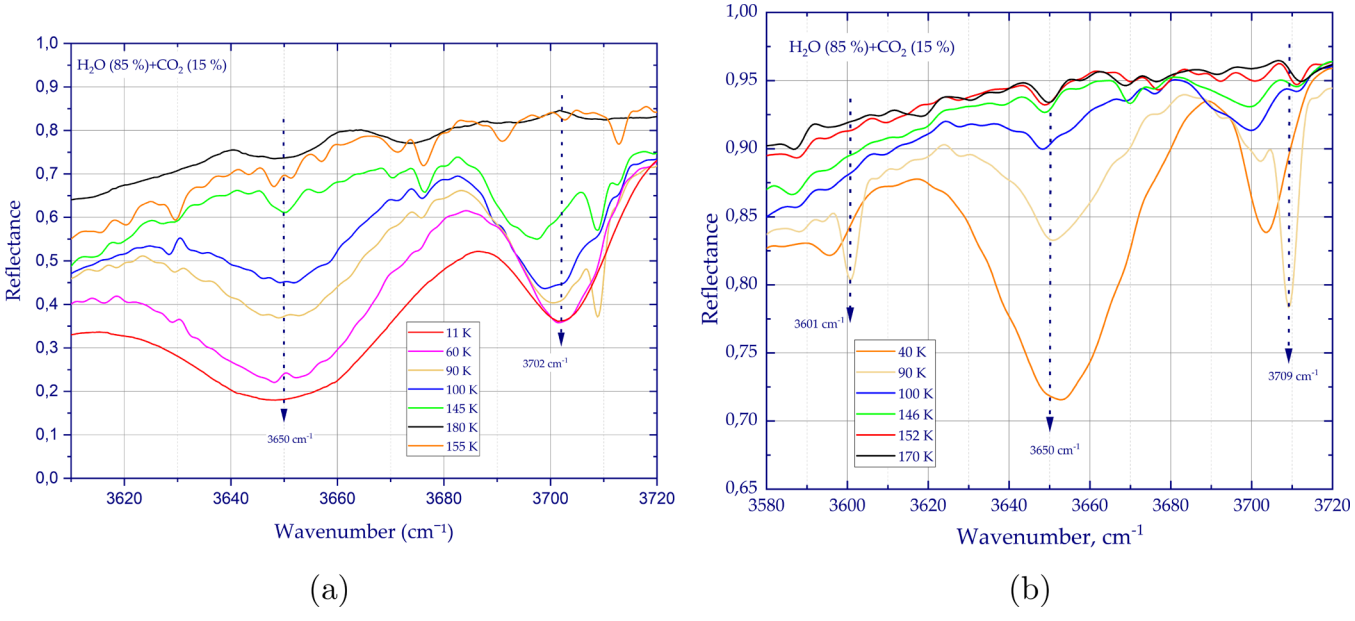

Figure 3. FTIR spectra of H_2O:CO_2 mixtures with 15% of CO_2 upon warming of the samples deposited at 11 K (panel a) and at 40 K (panel b).

https://doi.org/10.1021/acsomega.4c08342
ACS Omega 2025, 10, 1237−1248

this mixture. The substantial differences in the spectra from the same mixture deposited at different temperatures are worth mentioning. The warming of the sample shown in Figure 3b to 90 K apparently leads to the formation of the segregated CO_2 groups. These groups resemble the bands of pure solid CO_2 at 3601 and 3710 cm^{-1}. Nevertheless, the significant reduction of the CO_2 bands demonstrated in Figure 3b indicates that most of the CO_2 molecules sublimate at around 100 K.

To complement the experiments, we calculated the vibrational properties of the models of the mixtures under study, proposing different possible structures (Figure 12) that could be responsible for the observed peaks. We have found the minimum energy structures of the model complexes that could reflect the possible interactions of CO_2 and H_2O in the mixture. These theoretical calculations are not aimed at achieving a perfect match in frequency over the course of the experiment. The goal is to develop a model for possible formation mechanisms of different structures in H_2O:CO_2 mixtures that could explain the particular characteristics of their IR spectra.

Figure 4 shows the calculated fundamental vibrational peaks of the model structures in the region of 3450−3950 cm^{-1}. The

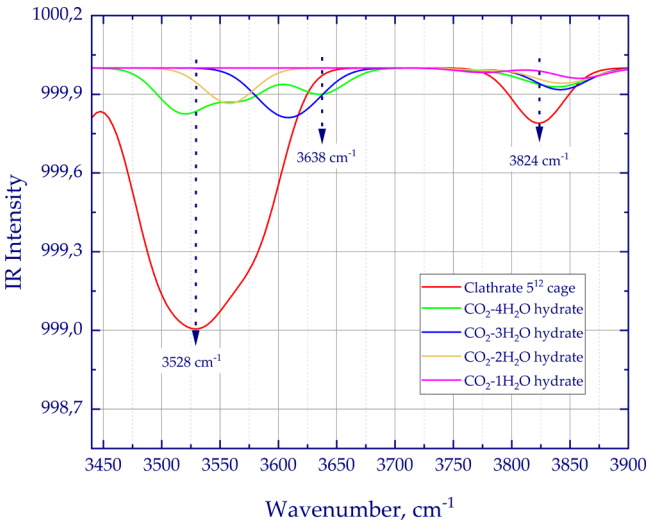

Figure 4. Calculated vibrational spectra of possible model structures formed in the mixtures of water and carbon dioxide in the regions of the H_2O stretching bands.

spectra indicate the differences in the positions of the peaks from different complexes and the broadening of the bands with an increasing number of water molecules. The characteristic band of the clathrate small cage 5^{12} shows broad features at around 3528 and 3824 cm^{-1} from hydrogen-bonded OH vibrations and dangling OH, respectively. Three bands are observed for the CO_2-$4H_2O$ complex at 3520, 3560, and 3650 cm^{-1}, corresponding to the region of the hydrogen-bonded OH absorption band. This model complex is also characterized by the feature at 3850 cm^{-1} corresponding to vibrations from dangling OH bonds. Notably, the band around 3650 cm^{-1} is assigned as the vibration of OH interacting with CO_2. Since the calculated vibrational spectra are obtained within the harmonic approximation, we cannot observe the combination bands of CO_2 in this region. Nevertheless, Figure 4 reflects the influence of interaction with the guest molecule on the stretching vibration absorption band of the water. Additionally, the observed broadening of the bands from the CO_2:H_2O mixtures could arise because of the wide structural variety of the formed complexes and their possible intramolecular interactions.

The most intensive infrared band of CO_2 is produced by C═O asymmetric stretching vibrations and falls near 2341 cm^{-1} for pure CO_2 ice (Figure 5a). The band in the mixtures is red-shifted from the pure material value to 2325 cm^{-1} and broadened to 2380 cm^{-1}. Subtle differences are observed in the band shape and position for different concentrations. However, the mixture with 5% CO_2 is characterized by a narrower band with split peaks at around 2335 and 2349 cm^{-1}, corresponding to the features of clathrate hydrates.[8,14]

The calculated vibrations shown in Figure 5b indicate that the band broadening from 2341 to 2380 cm^{-1} could appear due to the vibrations of clusters, CO_2 complexes with H_2O, and clathrates formed during the deposition of the samples. The calculated peaks from two clathrate cages are found at 2332 and 2410 cm^{-1} for $5^{12}6^2$ and 5^{12} cages, respectively. The vibrational bands of clusters of 1−5 CO_2 molecules in water solution appear at around 2367 cm^{-1} and have no shift relative to the increasing cluster size. It was also displayed in ref 32 that the increased size of the clusters up to 13 molecules led to the slight shift of the peak positions to higher frequencies up to 2367.7 cm^{-1} (Table 1). Furthermore, the position of CO_2−H_2O shows a size dependence. The peak position of the vibration from the CO_2-$4H_2O$ complex at 2382 cm^{-1} experiences the strongest blueshift of about 16 cm^{-1} from the bands of smaller complexes at 2368 cm^{-1}. Thus, we can assign the features in the region 2360−2380 cm^{-1} arising from the vibrations of CO_2 polyagregates of different sizes and their interaction with H_2O.

The $^{13}CO_2$ asymmetric stretching fundamental band is found near 2280 cm^{-1} for all the mixtures except for the 5% concentration (Figure 5a) experiencing the 4 cm^{-1} redshift from the pure CO_2 peak position. This band is caused by the same vibrational mode as the 2341 cm^{-1} band but is shifted to a lower frequency by the larger mass of the 13C atom. The width of the $^{13}CO_2$ band is narrower than the corresponding $^{12}CO_2$ band since the vibration is decoupled from the other CO_2 molecules in the matrix. The presence of guest molecules lowers its frequency similarly to that observed for the $^{12}CO_2$ band in the mixture with water.

The position and width of the CO_2 asymmetric stretch band are also temperature-dependent. Figure 6 illustrates this band as a function of temperature. The ice was deposited at 11 K (Figure 6a) and 40 K (Figure 6b) and warmed at a rate of 2 K/min to temperatures up to 180 K. The structures formed during condensation and warming of the samples with 15% CO_2 are essentially different concerning the deposition temperature. The spectra from the mixture condensed at 11 K display subtle differences with increasing temperature. However, a blueshift toward 2373 cm^{-1} was observed at 90 K. It then transformed into the splitting band appearing at 2335 and 2349 cm^{-1} at the temperature of 145 K. This splitting of the CO_2 stretching band and the peak positions correspond to the clathrate hydrate features according to the literature.[8,14,33] Notably, the peak at 2335 cm^{-1} assigned to the large $5^{12}6^2$ cages of the clathrate structure appeared in the spectra even at 11 K and remained constant up to 145 K. Besides, Ghosh et al.[22] reported the peak of clathrate hydrates observed in their mixtures deposited at 10 K and 10^{-10} mbar at 2346 cm^{-1} for different concentrations of CO_2 during deposition and after annealing up to 120 K for 48 h. On the

https://doi.org/10.1021/acsomega.4c08342
ACS Omega 2025, 10, 1237−1248

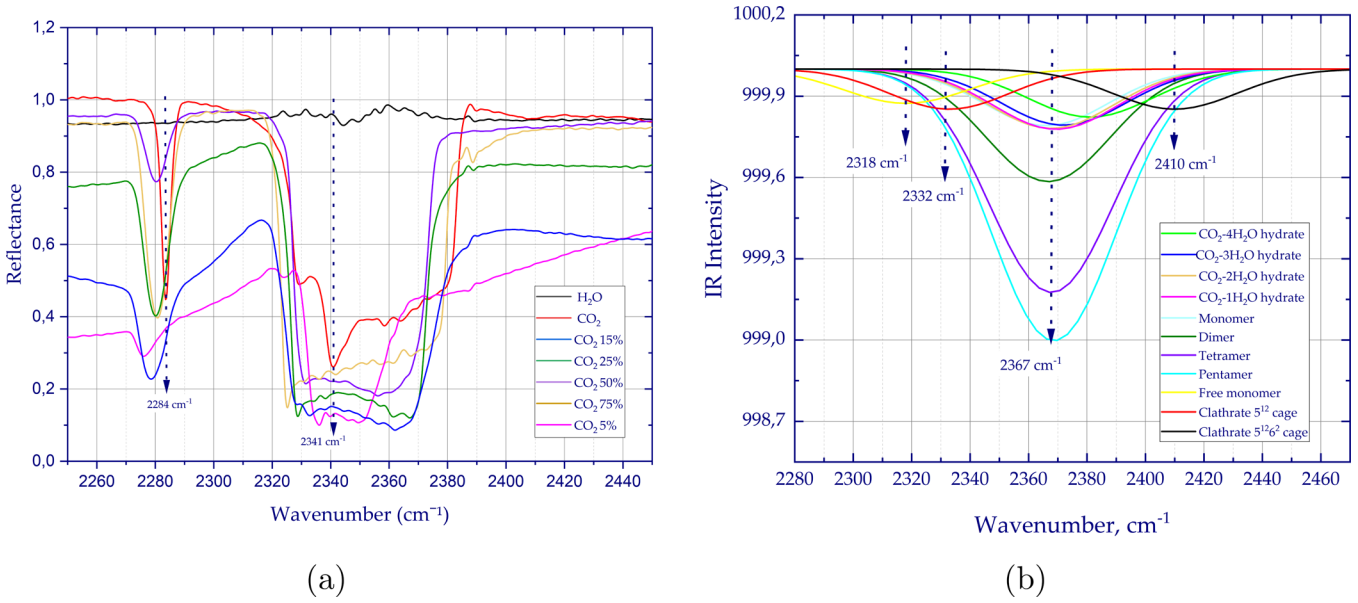

Figure 5. FTIR spectra of H_2O:CO_2 mixtures with different concentrations at 11 K (a) and calculated vibrational spectra of possible model structures formed in the mixtures of water and carbon dioxide (b).

contrary, in the present work, we suppose that clathrate hydrates could be formed during deposition of the 5% mixture at 10 K as well as after annealing of the 15% mixture to temperatures above 100 K and up to 145 K. Moreover, we observed the formation of both cages during deposition and upon annealing to 145 K. Additionally, the peak at around 2342 cm^{-1} at 155 K could be assigned either to the small cages of clathrates that remained after structural transformation in water or to the small polyaggregates monomers, dimers, and trimers of CO_2 molecules that remained after disruption of the cage.

The spectra of the mixture deposited at 40 K in Figure 6b display that the bandwidth decreases as the temperature increases. Increasing temperature leads to the steady shift of the band peak to a lower frequency at 2340 cm^{-1} assigned as the stretching vibration of the CO_2 in the crystalline phase. Therefore, it is supposed that for the mixtures with 15% of CO_2 deposited at 40 K, the segregation process prevails over the formation of clathrate hydrates. At temperatures above 80 K, the CO_2 molecules, due to their increased mobility, form pure CO_2 domains in the crystalline phase and large polyaggregates during deposition. Further warming causes the sublimation of polyaggregates and the formation of an ice mixture with isolated CO_2 domains trapped in the pores up to temperatures of H_2O structural transformations around 150 K.

The band at around 2382 cm^{-1} could be assigned to a weakly polarized longitudinal optical (LO) phonon mode of the CO_2 stretching mode.[34] Ovchinnikov and Wight[34] observed the transverse optical (TO) and LO modes of the CO_2 stretching mode split at 2344 and 2381 cm^{-1}, respectively, due to the crystalline nature of the CO_2 ice. It could possibly correspond to the stretching vibrations of large CO_2 polyaggregates formed during the deposition and further annealing.

As seen from Figure 6, mixed CO_2:H_2O ices demonstrate complex behavior at temperatures between 60 and 145 K. Significant segregation of CO_2 from the water ice matrix is observed during the deposition of these ices at temperatures of 40 K and above. Below this temperature, CO_2 is distributed homogeneously throughout the ice matrix, interacting with water molecules and forming clathrate structures. Additionally, warming of CO_2:H_2O ices from 11 K to higher temperatures leads to formation of polyaggregates of different sizes and clathrate hydrates, which trap CO_2 molecules inside the cage until the water sublimation temperatures. At the same time, warming of the samples from 40 K and higher leads to the segregation of carbon dioxide into isolated groups in the crystalline phase. Thus, the deposition temperature must be >40 K for CO_2 segregation/clustering.

The vibrational characteristic peak positions of CO_2 in different states and forms are presented in Table 1.

Mass Spectroscopy and Pressure Control. The pressure−temperature (PT) diagram in Figure 7 displays the desorption ranges of the formed structures in the H_2O:CO_2 mixtures of different concentrations. The desorption of the samples in the range from 85 to 105 K is associated with the "normal" sublimation of CO_2 at the operating pressure of P = 0.5 μTorr.[37] The second range, from 141 to 150 K, corresponds to CO_2 desorption during the phase transition from amorphous solid water to a cubic ice crystal structure. The third broad range of the diagram, from 165 to 187 K, is related to the complete sublimation of the sample due to the water sublimation and cosublimation of CO_2 molecules.

The PT diagram reflects the structural transformations that occurred in the samples upon warming depending on the mixture ratio. It is shown that the H_2O:CO_2 mixture with 5% CO_2 does not sublimate at first-range temperatures around 95 K. Sublimation of CO_2 molecules from this mixture is observed only in the second and third ranges. Notably, the sample sublimation temperature range is significantly broadened compared to the range observed from the mixture with 75% CO_2. Thus, the pressure control diagram supports the earlier hypothesis based on the IR spectra that the CO_2 molecules are already entrapped in clathrate hydrates during deposition of the 5% CO_2 mixture. According to Figure 7, we can suppose that for the mixture with 75% CO_2, the molecules of carbon dioxide are fully desorbed at temperatures lower than 100 K, and the water sublimation is fast and takes place in the narrow

https://doi.org/10.1021/acsomega.4c08342
ACS Omega 2025, 10, 1237−1248

Table 1. Carbon Dioxide Vibration Band Positions in Different Physical States[a]

CO_2 gas, cm^{-1}	CO_2 ice, cm^{-1}	H_2O:CO_2 complexes, cm^{-1}	CO_2 Clathrate, cm^{-1}	CO_2 clusters, cm^{-1}	mode
2360.0; 2341.0[a]	2343.3 (cryst)[a]; 2343.0 (cryst)[b]; 2340.0[g]; 2329.0 (amorph)[c]	2345.0[c]; 2338.8[a]; 2337.4[a] 2357.0; 2382.0[g]; 2369.3 (calc)[g]	2347.0; 2336.0[f]; 2347.0; 2336.5[g]; 2347.0; 2334.0[b]; 2349.3; 2336.3[g]	Monomer 2345.0; 2340.0; 2339.1[h]; 2365.0 (calc)[g]; Dimer 2346.3; 2382.6 (calc)[h]; 2346.5[i]; 2347.7; 2342.0; 2239.9[i]; 2366.7; 2367.3 (calc)[g]; Trimer 2343.0; 2353.0[h]; 2367.6 (calc)[g]; Tetramer 2367.8 (calc)[g]; Oligomers: 6−2353.6, 7−2356.3, 9−2358.7, 10−2361.2, 11−2361.8, 12−2364.3, 13−2367.7 [j]	ν_3^{12C}
2283.0[a]	2282.4[a]; 2281.0[b]; 2283.7[g]	2277.5[a]; 2277.8[a]; 2283.7[g]	2271.3; 2280[f]; 2272; 2281[e]; 2272; 2280[b] 2276[g]	Monomer 2279.5; 2274.7; 2273.7[h]; Dimer 2282; 2276.5; 2274.5[h]	ν_3^{13C}
3704.0[a]; 3726.0[b]	3707.5[a]; 3706.0[b]; 3711.5[g]	3702.1; 3707.7; 3695; 3704.0[g]	3703.4; 3692.7[f]; 3702; 3693[b]; 3697.3[g]	Monomer 3796.8−3699.5[h]	$\nu_1 + \nu_3$

[a] a - [20]; b - [33]; c - [13]; d - [15]; e - [14]; f - [8]; g - this work; h - [35]; i - [36]; j - [32].

range from 165 to 175 K. Therefore, it could be an indicator that neither enclathration nor segregation happens in the 75% CO_2 75% samples.

Moreover, some CO_2 desorption is observed at low temperatures around 95 K for the mixed ice with concentrations of 10−25%. Hence, some CO_2 molecules in such mixtures can diffuse through the porous ice structure and desorb at its sublimation temperature, while some carbon dioxide is entrapped in clathrate cages and stays in the sample until complete desorption of the film. Netsu and Ikeda-Fukazawa[21] observed similar effect for their samples with the approximately 34% concentration deposited at 42 K and sublimated in the temperature range of 82−102 K.

Figure 8a shows the mass spectra of the H_2O:CO_2 mixture with 15% CO_2 deposited at 11 K during sublimation, characterized by a pressure increase in the vacuum chamber. It can be clearly seen that most of the CO_2 molecules, about 80%, sublimate at an uncommon temperature of around 144 K and a little desorb at 93 K. The tiny portion of CO_2 leaves the sample at 172 K, coupled with water ice sublimation. The difference in the mass spectra of the mixture with 5% CO_2 is that more CO_2 molecules desorb at 172 K and fewer desorb at 98 K compared to 15% CO_2. This can be explained by the assumption that more clathrate hydrates were formed in a 5% mixture during deposition and did not cease to exist during warming. This could be another piece of evidence for the possible formation of clathrate hydrates in H_2O:CO_2 mixtures up to 25% CO_2.

Refractive Index. We determined the refractive indices of the thin films for different concentrations of CO_2 deposited at temperatures T = 11 K, T = 45 K, T = 80 K, and T = 110 K. Figure 9a clearly demonstrates that the refractive index increases with the concentration of CO_2 in the mixture deposited at the same temperature of T = 11 K with the highest value for the 75% of CO_2. It could indicate the growth of the structures that are somewhat different than pure CO_2 ice due to the interactions with water molecules. According to the analysis of vibrational spectra, the dependence of refractive indices on the concentration of CO_2 molecules reflects the variety of structures formed during deposition and is consistent with the observations we made from the PT diagram.

Figure 9b compares the refractive indices of the H_2O:CO_2 mixture with 15% CO_2 deposited at four different temperatures (11, 40, 80, and 110 K) and of pure water and carbon dioxide. The mixture and pure CO_2 are characterized by a significant temperature-based increase in the refractive index. The maximum observed refractive index of the mixture is determined at 80 K, followed by the substantial reduction of n at 130 K. The pattern is consistent with the data provided by other authors[38−40] and reflects the essential structural differences in the samples. The increasing refractive index of the mixture is indicative of the formation of denser morphologies and may correspond to the transition from an amorphous solid state at lower temperatures to a crystalline state at higher temperatures. Refractive indices of pure water increase as the temperature increases, which is observed for CO_2, albeit not drastically. This pattern also resembles the structural transformations in the water during warming and corresponds to the phase transition from amorphous solid water to cubic ice at around 140 K.

Thus, based on the analysis using FTIR, mass spectrometry, temperature-programmed desorption (TPD), and DFT calculations, we can suggest three different types of structures

https://doi.org/10.1021/acsomega.4c08342
ACS Omega 2025, 10, 1237−1248

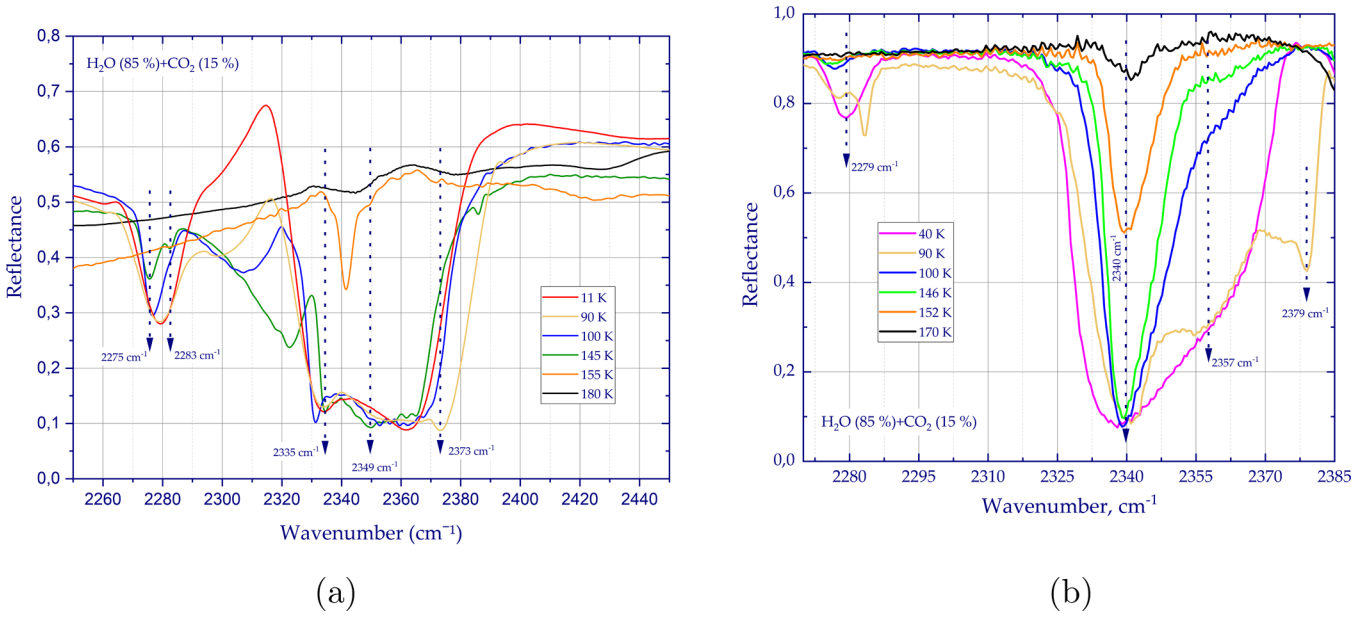

Figure 6. Temperature-dependent FTIR spectra of the H_2O:CO_2 = 15% mixture deposited at 11 K (a) and at 40 K (b) and warmed to 180 K.

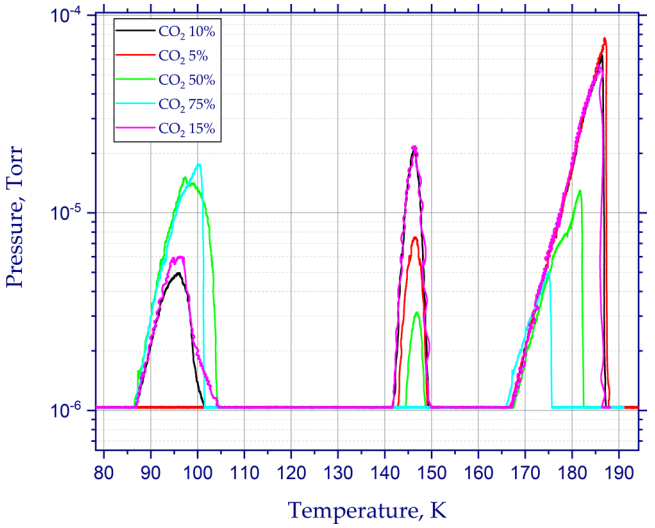

Figure 7. PT diagram of desorption for the H_2O:CO_2 mixtures of different concentrations deposited at 11 K.

formed in different mixtures. In the 75% CO_2 mixture, segregated groups of CO_2 molecules likely form already during deposition at 11 K subsequently interacting with amorphous water ice via the dangling OH bonds of H_2O. Similarly, the 15% CO_2 mixture deposited at 40 K, after warming up to 90 K, also exhibits characteristics of segregated CO_2 groups. The second type of structure is characterized by the formation of CO_2 polyagglomerates of different sizes trapped within the pores. This structure is observed in mixtures with 10 to 50% CO_2 concentration deposited at 11 K. Notably, after warming these mixtures to temperatures above 100 K, they begin to display the features of clathrate hydrates. A different behavior is observed for the third type of structure, found in the 5% CO_2 mixture deposited at 11 K. In this case, clathrate hydrates are already formed during the deposition, and the CO_2 molecules sublimate completely upon water sublimation at temperatures around 185 K, which is higher than the normal sublimation temperature of pure water ice at a pressure of P = 0.5 μTorr.

MATERIALS AND METHODS

The thin films of H_2O:CO_2 mixtures are prepared using the physical vapor deposition (PVD) technique.[41] The deposition was performed at T = 11 K on a special, gold-coated substrate of a semiautomatic cryovacuum spectrophotometer unit, as shown in Figure 10. The PVD method is well-known as a practical approach for the formation of thin films with controlled structural phase states.[42−44] It is usually recommended to study the optical and physical properties of the materials at low and ultralow temperatures.[44−47] The Extorr XT100 gas analyzer (Extorr Inc., USA), a quadrupole residual gas analyzer, and a heating element built into the substrate allowed us to determine the film composition during sublimation. The present work obtained spectra in the 11−200 K temperature range at a pressure of P = 0.5 μTorr. The film thickness remained constant throughout the experiments at all of the condensation temperatures.

An automated temperature control module made with the LabView software package (National Instruments, USA) is another important feature of the unit. This module connects the cooling substrate of the Gifford-McMahon machine, the heater, the temperature sensor DT-670, and the PID controller of the LakeShore 325 thermal controller (LakeShore, USA). Furthermore, it helps to reach the required temperatures more quickly and further stabilize them near the reference to determine the spectral characteristics. In addition, as soon as the reference point is reached, the module switches off the Gifford-McMahon machine to avoid vibrational oscillations from the operating machine. The spectral characteristics of the samples were detected using the FSM 2203 FTIR spectrometer (INFRASPEK, Russia) with a maximum spectral resolution of 0.125 cm^{-1} and a spectral range of 370−7800 cm^{-1}. For a more detailed description of the experimental setup and methodology, please refer to our earlier works.[48−50]

The refractive index and thickness of thin films deposited on the substrate are determined by using the interference patterns obtained from the two beams of a semiconductor laser formed by fission and detected by using a P25A photomultiplier tube (Sens-Tech, UK). The angles of incidence of the two beams

https://doi.org/10.1021/acsomega.4c08342
ACS Omega 2025, 10, 1237−1248

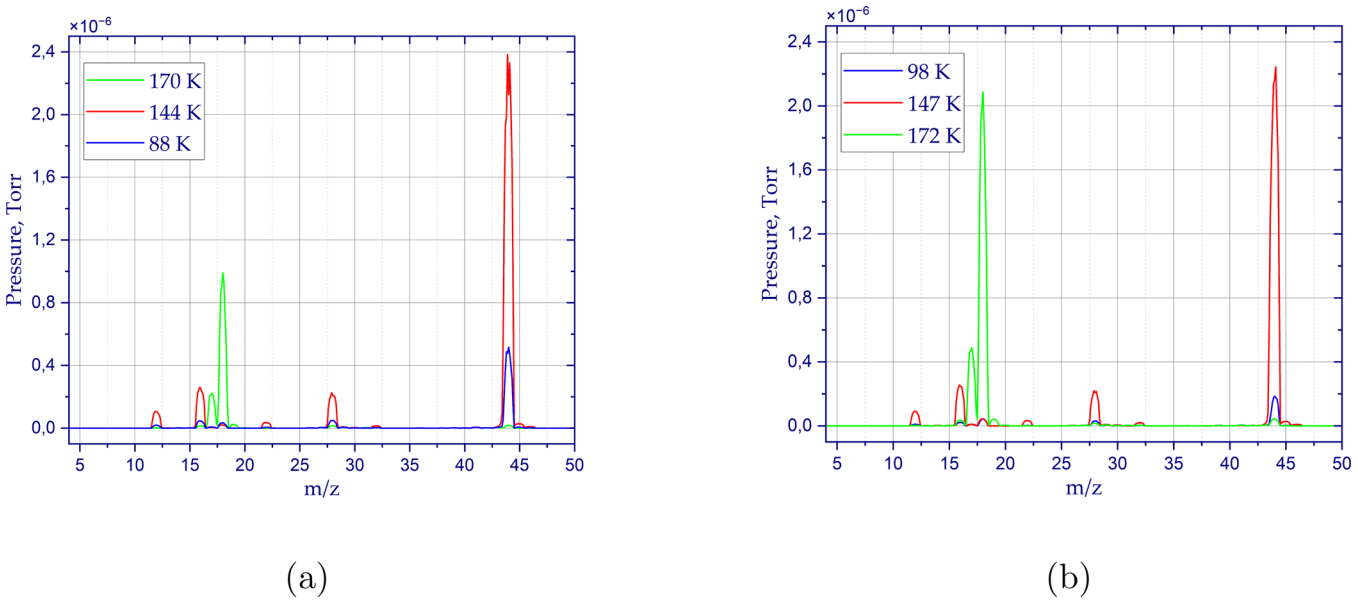

Figure 8. Mass spectra of the H_2O:CO_2 mixture with (a) 15% of CO_2 deposited at 11 K and (b) 5% of CO_2 deposited at 11 K.

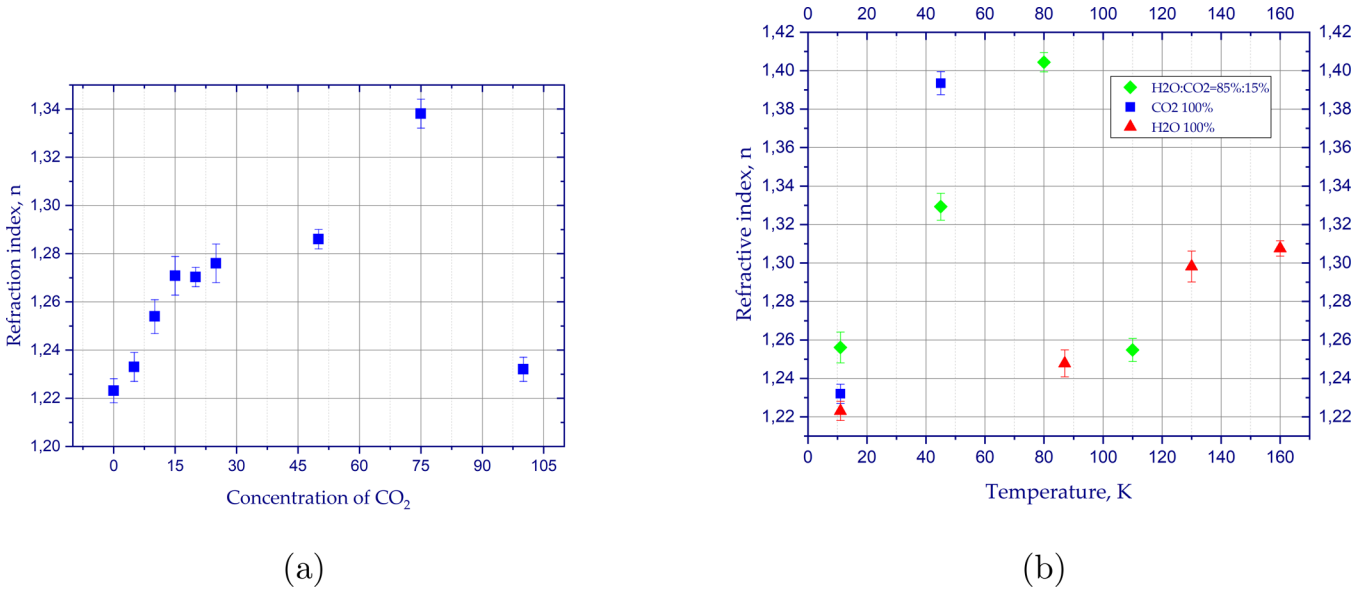

Figure 9. (a) Refractive indices of the mixtures depending on the concentration of CO_2; (b) refractive indices of the H_2O:CO_2 mixture with 15% of CO_2 deposited at different temperatures compared to the values from pure carbon dioxide and water ices.

are $\alpha_1 \approx 0°$ and $\alpha_2 \approx 45°$. The laser wavelength is $\lambda = 406$ nm, and the maximum sensitivity of the photomultiplier tube is in the range of about 400 nm, as well, which is important for obtaining high-quality interference patterns. The refractive indices are calculated then using the following formula:

$$n = \sqrt{\frac{\sin^2 \alpha_2 - \left(\frac{t_1}{t_2}\right)^2 \sin^2 \alpha_1}{1 - \left(\frac{t_1}{t_2}\right)^2}} \quad (1)$$

where t_1 and t_2 are the periods and α_1 and α_2 are the angles of incidence of the first and second lasers, respectively. The applied method is described in more detail in our earlier publications.[49−53]

CO_2 of 99.999% purity (IHSAN TEHNO-GAS LLP, Almaty, Kazakhstan) was used in the experiments. It had a maximum oxygen fraction not exceeding 0.0005%, water vapors not exceeding 0.0007%, and distilled water with a mass fraction of residue after evaporation not exceeding 0.005% of the volume was used in the experiments.

To prepare the mixtures with different concentration ratios of the substances in necessary proportions, we relied on Dalton's law of partial pressure. We followed the two-step approach for thin film formation. In the first stage, we created the mixture inside the drained leakage system by sequentially injecting the mixture components, starting from the one with a lower saturated vapor pressure. The ratio of the components was controlled by the pressure values. The mixture was then injected into the vacuum chamber and deposited on the substrate.

Figure 11 demonstrates the optimized geometries of CO_2 molecules inside the two types of cages (5^{12} and $5^{12}6^2$), which

https://doi.org/10.1021/acsomega.4c08342
ACS Omega 2025, 10, 1237−1248

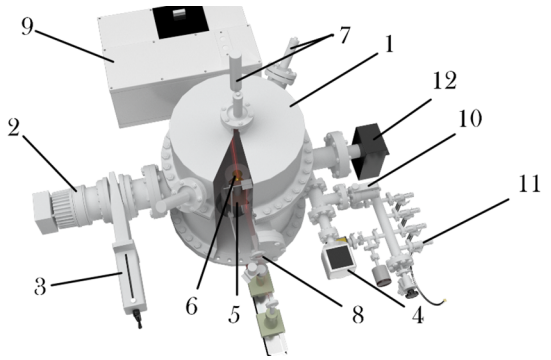

Figure 10. Cryovacuum condensation experimental setup: (1) vacuum chamber, (2) vacuum pump Turbo V-301, (3) vacuum gate valve CFF-100, (4) pressure detector FRG-700, (5) Gifford-McMahon refrigerator, (6) substrate, (7) photo multiplier, laser interferometer, (8) light source, optical channel, (9) IR-spectrometer, (10) high-precision gas supply leak into the chamber; (11) gas leak into the mixture production system; (12) Extorr XT100.

usually form the clathrate hydrate of carbon dioxide. In this study, we used first-principles calculations by DFT methods to improve the accuracy of the obtained vibrational spectra, considering corrections for dispersion interactions (D3BJ). We also found the minimum energy structures of the model complexes. They can be formed during the deposition and annealing of the mixtures. In Figure 12, we show the considered models of CO_2:H_2O complexes and CO_2 clusters.

Quantum mechanical calculations were carried out in the Orca-5.0.2 package with the following main parameters: B3LYP was chosen as the density functional using the correction for the dispersion of Grimme atoms with Becke–Johnson damping (D3BJ); for all atoms, `zora-def2-TZVPP` recontracted Gaussian-type basis sets were used with auxiliary SARC/J Coulomb-fit basis sets for the sphere chain/identity resolution method (RIJCOSX); improved integration accuracy (defgrid3 and IntAcc 6.0) and a dense self-consistent field were used as convergence criteria; and the conductive polarizable continuum model (CPCM) with water parameters was applied in some calculations to place the system under study in a suitable volumetric solution environment.

The positions of oxygen atoms in the water molecules were experimentally determined via X-ray diffraction analysis.[54,55] The coordinates of the hydrogen atoms in the sI unit cell were assigned by applying the ice rules, ensuring that the net dipole moment of the unit cell is zero and that the proton configuration corresponded to the lowest potential energy state. We employed the Orca-5.0.2 software package to compute the vibrational frequencies based on the geometries obtained from periodic calculations. The B3LYP hybrid functional was chosen for its reliable balance between computational cost and accuracy in conjunction with the zora-def2-TZVPP basis set. Vibrations were calculated within the harmonic approximation using a cluster consisting of one small and one large cage to replicate the atomic arrangement in the crystal. The geometry relaxation of the periodic structure produced a unit cell lattice parameter of a = 11.784 Å for the equilibrium geometry of saturated CO sI clathrate, which shows good agreement with the experimental value of a = 11.893 Å reported by Udachin et al.[54] The slight difference between the calculated and experimental values can be attributed to thermal expansion effects.

The average distances obtained for the zero-pressure equilibrium structure are 1.171 Å for C═O, 0.999 Å for the O–H covalent bond, 1.711 Å for hydrogen bonds, and 2.710 Å for the O–O intermolecular distance. The C═O bond distance is in good agreement with experimental values around 1.161 Å.[54] As for the free CO_2 molecule, the calculated bond distance is 1.172 Å and the experimental value is 1.162 Å. The data obtained highlight the accuracy and consistency of our computational methods as well as the structural similarity between clathrate hydrates and ice.

CONCLUSIONS

We investigated different morphologies in the thin films of H_2O:CO_2 mixtures with different concentration ratios prepared using the PVD method at deposition temperatures ranging from 11 to 180 K. According to the analysis based on FTIR, mass spectroscopy, TPD, and DFT calculations, we suppose that H_2O:CO_2 mixtures can form a wide variety of structures under interstellar-like conditions depending on the CO_2 concentration and deposition temperature, including clathrate hydrates, polyaggregates of different sizes, and segregated groups trapped within the pores.

First of all, we observed the peaks at 2335 and 2349 cm^{-1} assigned by us to the clathrate hydrates formed in the 5% CO_2 films already during deposition at 11 K. Additionally, the absence of the dangling OH peak at around 3650 cm^{-1} and substantial redshift of the combination band to 3698 cm^{-1} could also indicate clathrate formation in this mixture. Furthermore, the mixture with 15% CO_2 deposited at 11 K can form clathrate hydrates either during deposition or during the warming to 145 K. We observed three kind of structures formed in the mixtures with 10 to 50% concentration: clathrate hydrates, polyaggregates of different sizes, and segregated groups of CO_2 molecules. The 15% CO_2 sample condensed at

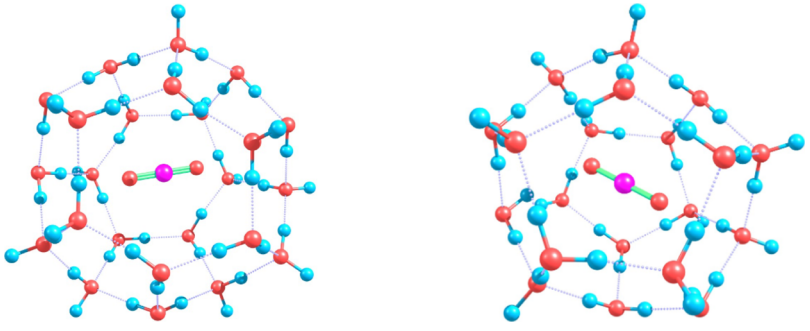

Figure 11. Optimized configuration of the CO_2 molecule inside a $5^{12}6^2$-type cell (left); inside a 5^{12}-type cell (right).

https://doi.org/10.1021/acsomega.4c08342
ACS Omega 2025, 10, 1237−1248

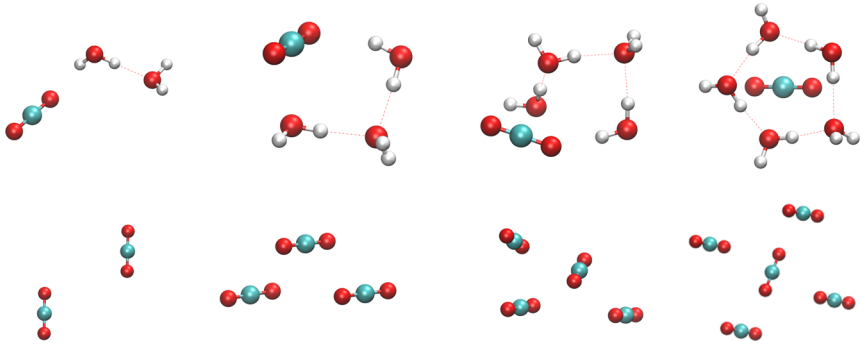

Figure 12. Optimized geometries of model complexes representing the possible H_2O:CO_2 complexes (top) and cluster (down) structures in CO_2:H_2O mixtures of different concentrations.

40 K is characterized only by the formation of segregated groups of CO_2 trapped within the pores of amorphous solid water.

Moreover, the PT diagram and mass spectrometry data reveal distinct sublimation behaviors for different CO_2 concentrations in the H_2O:CO_2 ice mixtures. The 5% CO_2 mixture exhibits a broadened sublimation temperature range and lacks CO_2 desorption at lower temperatures (around 95 K), supporting the formation of clathrate hydrates during deposition. In contrast, the 75% CO_2 mixture shows complete CO_2 desorption below 100 K and rapid water sublimation, suggesting neither clathrate formation nor significant CO_2 trapping. The 15% CO_2 mixture displays a significant portion of CO_2 sublimating at 144 K, indicating the presence of clathrate hydrates, while a small fraction cosublimates with water at 172 K. These findings, combined with the observation of some CO_2 desorption at lower temperatures for mixtures with 10−25% CO_2, suggest a combination of clathrate formation and diffusion through porous ice structures depending on the CO_2 concentration.

Thus, we have demonstrated two possible mechanisms, segregation into CO_2 groups and enclathration in the cages, for the formation of the structures responsible for the uncommon sublimation of CO_2 at around 145 K in the mixtures with water, depending on the concentration ratio and deposition temperature.

In addition, research on the concentration and temperature dependence of the refractive indices displayed the essential structural differences observed in the samples at various concentration ratios. Higher concentrations of CO_2 in the CO_2:H_2O ice mixtures lead to an increase in the refractive index, indicating the growth of denser structures compared to pure CO_2 ice. This dependence of the refractive index on the CO_2 concentration reflects the diverse range of structures formed during deposition, consistent with observations from vibrational spectra and the PT diagram.

AUTHOR INFORMATION

Corresponding Authors

Aliya Tychengulova − *Fesenkov Astrophysical Institute, 050020 Almaty, Kazakhstan; Laboratory of Engineering Profile, Satbayev University, 050013 Almaty, Kazakhstan;* orcid.org/0000-0002-1849-1560; Email: a.tychengulova@gmail.com

Darkhan Yerezhep − *Faculty of Physics and Technology, Al-Farabi Kazakh National University, 050040 Almaty, Kazakhstan;* Present Address: Institute of Energy and Mechanical Engineering, Satbayev University, Satbayev str. 22, 050013 Almaty, Kazakhstan; orcid.org/0000-0002-2232-2911; Email: darhan_13@physics.kz

Authors

Karakoz Katpayeva − *Fesenkov Astrophysical Institute, 050020 Almaty, Kazakhstan; Natural Sciences Research Institute, Ahmet Yassawi University, 161200 Turkestan, Kazakhstan;* orcid.org/0000-0002-4867-4974

Saule Shomshekova − *Fesenkov Astrophysical Institute, 050020 Almaty, Kazakhstan*

Saltanat Ibragimova − *Fesenkov Astrophysical Institute, 050020 Almaty, Kazakhstan*

Oleg Golikov − *Faculty of Physics and Technology, Al-Farabi Kazakh National University, 050040 Almaty, Kazakhstan*

Dmitriy Sokolov − *Faculty of Physics and Technology, Al-Farabi Kazakh National University, 050040 Almaty, Kazakhstan; Faculty of Engineering and Information Technology, Almaty Technological University, 050012 Almaty, Kazakhstan;* orcid.org/0000-0001-7966-1140

Abdurakhman Aldiyarov − *Faculty of Physics and Technology, Al-Farabi Kazakh National University, 050040 Almaty, Kazakhstan;* orcid.org/0000-0002-5091-7699

Complete contact information is available at: https://pubs.acs.org/10.1021/acsomega.4c08342

Notes

The authors declare no competing financial interest.

ACKNOWLEDGMENTS

This research was funded by the Science Committee of the Ministry of Education and Science of the Republic of Kazakhstan (Grant No. AP14871603).

REFERENCES

(1) Fard, K.; Smith, I. Properties of water, carbon dioxide, and nitrogen ices in planetary surface environments. *Icarus* **2024**, *410*, No. 115895.

(2) Cao, P.; Wu, J.; Ning, F. Mechanical properties of amorphous CO2 hydrates: insights from molecular simulations. *Phys. Chem. Chem. Phys.* **2024**, *26*, 9388−9398.

(3) Yu, X.; Yu, Y.; Garver, J.; Li, J.; Hawthorn, A.; Sciamma-O'Brien, E.; Zhang, X.; Barth, E. Material properties of organic liquids, ices, and Hazes on Titan. *Astrophys. J. Suppl. Ser.* **2023**, *266*, 30.

(4) Ahrens, C.; Meraviglia, H.; Bennett, C. A Geoscientific Review on CO and CO2 Ices in the Outer Solar System. *Geosciences* **2022**, *12*, 51.

(5) Schiltz, L.; Escribano, B.; Muñoz Caro, G.; Cazaux, S.; del Burgo Olivares, C.; Carrascosa, H.; Boszhuizen, I.; González Díaz, C.; Chen,

https://doi.org/10.1021/acsomega.4c08342
ACS Omega 2025, 10, 1237−1248

Y.-J.; Giuliano, B.; et al. Characterization of carbon dioxide on Ganymede and Europa supported by experiments: Effects of temperature, porosity, and mixing with water. *Astron. Astrophys.* **2024**, *688*, A155.
(6) Ehrenfreund, P.; Dartois, E.; Demyk, K.; D'Hendecourt, L. Ice segregation toward massive protostars. *Astron. Astrophys.* **1998**, *339*, L17−L20.
(7) Dartois, E.; Schutte, W.; Geballe, T. R.; Demyk, K.; Ehrenfreund, P.; D'Hendecourt, L. Methanol: The second most abundant ice species towards the high-mass protostars RAFGL7009S and W 33A. *Astron. Astrophys.* **1999**, *33A* (342), L32−L35.
(8) Dartois, E.; Schmitt, B. Carbon dioxide clathrate hydrate FTIR spectrum. *Near infrared combination modes for astrophysical remote detection.* **2009**, *504*, 869−873.
(9) Baratta, G. A.; Palumbo, M. E.; Strazzulla, G. Laboratory and astronomical IR spectra: an experimental clue for their comparison. *Astron. Astrophys.* **2000**, *357*, 1045−1050.
(10) Hodyss, R.; Johnson, P. V.; Orzechowska, G. E.; Goguen, J. D.; Kanik, I. *Carbon dioxide segregation in 1:4 and 1:9 CO 2:H 2O ices* **2008**, *194*, 836−842.
(11) Öberg, K. I.; Fayolle, E. C.; Cuppen, H. M.; van Dishoeck, E. F.; Linnartz, H. *Quantification of segregation dynamics in ice mixtures.* **2009**, *505*, 183−194.
(12) Isokoski, K.; Bossa, J.-B.; Triemstra, T.; Linnartz, H. Porosity and thermal collapse measurements of H2O, CH3OH, CO2, and H2O:CO2 ices. *Phys. Chem. Chem. Phys.* **2014**, *16*, 3456−3465.
(13) Bernstein, M. P.; Cruikshank, D. P.; Sandford, S. A. Near-infrared laboratory spectra of solid H2O/CO2 and CH3OH/CO2 ice mixtures. *Icarus* **2005**, *179*, 527−534.
(14) Fleyfel, F.; Devlin, J. P. Carbon dioxide clathrate hydrate epitaxial growth: Spectroscopic evidence for formation of the simple type-II CO_2 hydrate. *Journal of Physics Conference Series.* **1991**, *95*, 3811−3815.
(15) Kumar, R.; Englezos, P.; Moudrakovski, I.; Ripmeester, J. A. Structure and composition of CO2/H2 and CO2/H2/C3H8 hydrate in relation to simultaneous CO2 capture and H2 production. *AIChE J.* **2009**, *55*, 1584−1594.
(16) Kieffer, H. *Spectral reflectance of CO2-H2O Frosts.* **1970**, *75*, 501.
(17) Smythe, W. D. *Spectra of Hydrate Frosts: Their Application to the Outer Solar System.* **1975**, *24*, 421−427.
(18) Seo, Y. T.; Lee, H. Structure and guest distribution of the mixed carbon dioxide and nitrogen hydrates as revealed by X-ray diffraction and C-13 NMR spectroscopy. *JOURNAL OF PHYSICAL CHEMISTRY B* **2004**, *108*, 530−534.
(19) Sandford, S. A.; Allamandola, L. J. *Physical and Infrared Spectral Properties of CO 2 in Astrophysical Ice Analogs.* **1990**, *355*, 357.
(20) Blake, D.; Allamandola, L.; Sandford, S.; Hudgins, D.; Freund, F. Clathrate Hydrate Formation in Amorphous Cometary Ice Analogs in Vacuo. *Science* **1991**, *254*, 548−551.
(21) Netsu, R.; Ikeda-Fukazawa, T. Formation of carbon dioxide clathrate hydrate from amorphous ice with warming. *Chem. Phys. Lett.* **2019**, *716*, 22−27.
(22) Ghosh, J.; Methikkalam, R. R. J.; Bhuin, R. G.; Ragupathy, G.; Choudhary, N.; Kumar, R.; Pradeep, T. Clathrate hydrates in interstellar environment. *Proc. Natl. Acad. Sci. U. S. A.* **2019**, *116*, 1526−1531.
(23) Vishwakarma, G.; Malla, B. K.; Reddy, K. P.; Ghosh, J.; Chowdhury, S.; Yamijala, S. S.; Reddy, S. K.; Kumar, R.; Pradeep, T. Induced Migration of CO2 from Hydrate Cages to Amorphous Solid Water under Ultrahigh Vacuum and Cryogenic Conditions. *J. Phys. Chem. Lett.* **2023**, *14*, 2823−2829.
(24) Ghosh, J.; Vishwakarma, G.; Kumar, R.; Pradeep, T. Formation and Transformation of Clathrate Hydrates under Interstellar Conditions. *Acc. Chem. Res.* **2023**, *56*, 2241−2252.
(25) Chen, B.; Sun, H.; Zheng, J.; Yang, M. New insights on water-gas flow and hydrate decomposition behaviors in natural gas hydrates deposits with various saturations. *Applied Energy* **2020**, *259*, No. 114185.
(26) Yang, M.; Sun, H.; Chen, B.; Song, Y. Effects of water-gas two-phase flow on methane hydrate dissociation in porous media. *Fuel* **2019**, *255*, No. 115637.
(27) Wells, J. D.; Majid, A. A.; Creek, J. L.; Sloan, E. D.; Borglin, S. E.; Kneafsey, T. J.; Koh, C. A. Water content of carbon dioxide at hydrate forming conditions. *Fuel* **2020**, *279*, No. 118430.
(28) Zhang, N.; Li, S.; Chen, L.; Guo, Y.; Liu, L. Study of gas-liquid two-phase flow characteristics in hydrate-bearing sediments. *Energy* **2024**, *290*, No. 130215.
(29) Guo, Z.; Chen, X.; Wang, B.; Ren, X. Two-phase relative permeability of hydrate-bearing sediments: A theoretical model. *Energy* **2023**, *275*, No. 127441.
(30) Hudgins, D.; Sandford, S.; Allamandola, L.; Tielens, A. Mid-and far-infrared spectroscopy of ices-Optical constants and integrated absorbances. *Astrophys. J. Suppl. Ser.* **1993**, *86*, 713−870.
(31) Gerakines, P. A.; Bray, J.; Davis, A.; Richey, C. The strengths of near-infrared absorption features relevant to interstellar and planetary ices. *Astrophysical Journal* **2005**, *620*, 1140.
(32) Oliaee, J. N.; Dehghany, M.; Moazzen-Ahmadi, N.; McKellar, A. Spectroscopic identification of carbon dioxide clusters:(CO 2) 6 to (CO 2) 13. *Phys. Chem. Chem. Phys.* **2011**, *13*, 1297−1300.
(33) Oancea, A.; Grasset, O.; Le Menn, E.; Bollengier, O.; Bezacier, L.; Le Mouélic, S.; Tobie, G. Laboratory infrared reflection spectrum of carbon dioxide clathrate hydrates for astrophysical remote sensing applications. *Icarus* **2012**, *221*, 900−910.
(34) Ovchinnikov, M. A.; Wight, C. A. Inhomogeneous broadening of infrared and Raman spectral bands of amorphous and polycrystalline thin films. *J. Chem. Phys.* **1993**, *99*, 3374−3379.
(35) Schriver, A.; Schriver-Mazzuoli, L.; Vigasin, A. A. Matrix isolation spectra of the carbon dioxide monomer and dimer revisited. *Vib. Spectrosc.* **2000**, *23*, 83−94.
(36) Dehghany, M.; Afshari, M.; Moazzen-Ahmadi, N.; McKellar, A. The cyclic CO2 trimer: Observation of a parallel band and determination of an intermolecular out-of-plane torsional frequency. *J. Chem. Phys.* **2008**, *128*, No. 064308.
(37) Bryson, C. E., III; Cazcarra, V.; Levenson, L. L. Sublimation rates and vapor pressures of water, carbon dioxide, nitrous oxide, and xenon. *J. Chem. Eng. Data* **1974**, *19*, 107−110.
(38) Satorre, M.; Domingo, M.; Millán, C.; Luna, R.; Vilaplana, R.; Santonja, C. Density of CH4, N2 and CO2 ices at different temperatures of deposition. *Planetary and Space Science* **2008**, *56*, 1748−1752.
(39) Luna, R.; Satorre, M.; Domingo, M.; Millán, C.; Santonja, C. Density and refractive index of binary CH4, N2 and CO2 ice mixtures. *Icarus* **2012**, *221*, 186−191.
(40) Baratta, G.; Palumbo, M. Infrared optical constants of CO and CO 2 thin icy films. *JOSA A* **1998**, *15*, 3076−3085.
(41) Li, X.-S.; Xu, C.-G.; Chen, Z.-Y.; Wu, H.-J. Hydrate-based pre-combustion carbon dioxide capture process in the system with tetra-n-butyl ammonium bromide solution in the presence of cyclopentane. *Energy* **2011**, *36*, 1394−1403.
(42) Liu, H.; Wang, J.; Chen, G.; Liu, B.; Dandekar, A.; Wang, B.; Zhang, X.; Sun, C.; Ma, Q. High-efficiency separation of a CO2/H2 mixture via hydrate formation in W/O emulsions in the presence of cyclopentane and TBAB. *Int. J. Hydrogen Energy* **2014**, *39*, 7910−7918.
(43) Horii, S.; Ohmura, R. Continuous separation of CO2 from a H2+CO2 gas mixture using clathrate hydrate. *Applied Energy* **2018**, *225*, 78−84.
(44) Nallakukkala, S.; Rehman, A. u.; Zaini, D. B.; Lal, B. Gas Hydrate-Based Heavy Metal Ion Removal from Industrial Wastewater: A Review. *Water* **2022**, *14*, 1171.
(45) Guerra, A.; Mathews, S.; Marić, M.; Servio, P.; Rey, A. D. All-Atom Molecular Dynamics of Pure Water−Methane Gas Hydrate Systems under Pre-Nucleation Conditions: A Direct Comparison between Experiments and Simulations of Transport Properties for the Tip4p/Ice Water Model. *Molecules* **2022**, *27*, 5019.
(46) Khan, M.; Warrier, P.; Peters, C.; Koh, C. Hydrate-Based Separation for Industrial Gas Mixtures. *Energies* **2022**, *15*, 966.

https://doi.org/10.1021/acsomega.4c08342
ACS Omega 2025, 10, 1237−1248

(47) Mohammadi, A. H.; Eslamimanesh, A.; Belandria, V.; Richon, D. Phase equilibria of semiclathrate hydrates of CO2, N2, CH4, or H2+ tetra-n-butylammonium bromide aqueous solution. *Journal of Chemical & Engineering Data* **2011**, *56*, 3855−3865.
(48) Golikov, O.; Yerezhep, D.; Akylbayeva, A.; Sokolov, D. Y.; Korshikov, E.; Nurmukan, A.; Aldiyarov, A. Cryovacuum setup for optical studies of astrophysical ice. *Sci. Rep.* **2023**, *13*, 21155.
(49) Sokolov, D. Y.; Yerezhep, D.; Vorobyova, O.; Ramos, M. A.; Shinbayeva, A. Optical studies of thin films of cryocondensed mixtures of water and admixture of nitrogen and argon. *Materials* **2022**, *15*, 7441.
(50) Yerezhep, D.; Akylbayeva, A.; Golikov, O.; Sokolov, D. Y.; Shinbayeva, A.; Aldiyarov, A. U. Analysis of vibrational spectra of tetrafluoroethane glasses deposited by physical vapor deposition. *ACS omega* **2023**, *8*, 19567−19574.
(51) Sokolov, D. Y.; Yerezhep, D.; Vorobyova, O.; Golikov, O.; Aldiyarov, A. U. Infrared analysis and effect of nitrogen and nitrous oxide on the glass transition of methanol cryofilms. *ACS omega* **2022**, *7*, 46402−46410.
(52) Tychengulova, A.; Capone, M.; Pitari, F.; Guidoni, L. Molecular Vibrations of an Oxygen-Evolving Complex and Its Synthetic Mimic. *Chemistry−A. European Journal* **2019**, *25*, 13385−13395.
(53) Tychengulova, A.; Aldiyarov, A.; Drobyshev, A. Molecular dynamics simulation of thermodynamic and transport properties of H-bonded low-temperature substances. *Low Temperature Physics* **2015**, *41*, 454−458.
(54) Udachin, K. A.; Ratcliffe, C. I.; Ripmeester, J. A. Structure, composition, and thermal expansion of CO2 hydrate from single crystal X-ray diffraction measurements. *J. Phys. Chem. B* **2001**, *105*, 4200−4204.
(55) Manakov, A. Y.; Dyadin, Y. A.; Ogienko, A. G.; Kurnosov, A. V.; Aladko, E. Y.; Larionov, E. G.; Zhurko, F. V.; Voronin, V. I.; Berger, I. F.; Goryainov, S. V.; et al. Phase diagram and high-pressure boundary of hydrate formation in the carbon dioxide- water system. *J. Phys. Chem. B* **2009**, *113*, 7257−7262.

https://doi.org/10.1021/acsomega.4c08342
ACS Omega 2025, 10, 1237−1248